Deamidation, but Not Truncation, Decreases the Urea Stability of a Lens Structural Protein, βB1-Crystallin†

Yung Hae Kim,‡,@ Deborah M. Kapfer,§ Jos Boekhorst,|| Nicolette H. Lubsen,|| Hans Peter Bächinger,⊥ Thomas R. Shearer,‡,§ Larry L. David,‡,§ Jimmy B. Feix,▽,@ and Kirsten J. Lampi*,§,@

Department of Animal Sciences, Oregon State University, Corvallis, Oregon 97331, Oral Molecular Biology, School of Dentistry, Oregon Health & Science University, Portland, Oregon 97239, Department of Biochemistry, University of Nijmegen, Nijmegen, The Netherlands, Shriner's Hospital for Children, Portland, Oregon 97201, and National Biomedical EPR Center, Medical College of Wisconsin, Milwaukee, Wisconsin 53226

Received June 12, 2002; Revised Manuscript Received September 16, 2002

ABSTRACT: Crystallins, the major structural proteins in the lens of the eye, are maintained with little turnover throughout the lifetime of the host. With time, lens crystallins undergo post-translational modifications that may play an important role in loss of vision during aging and cataract formation. Specific modifications include deamidation and truncation. Urea-induced denaturation was studied for recombinantly expressed wild-type βB1 (WT), the deamidated mutant (Q204E), an N-terminally truncated mutant (βB1(ΔN41)), and other truncated versions of these proteins generated by calpain II digestion. Tryptophan fluorescence was used to monitor loss of global tertiary structure. Loss of secondary structure was followed by circular dichroism, and electron paramagnetic resonance site-directed spin labeling was used to monitor loss of tertiary structure selectively in the N-terminal domain. Our results indicated that the deamidated mutant was significantly destabilized relative to WT. Q204E showed a two-step denaturation curve with transitions at 4.1 and 7.2 M urea, whereas denaturation of WT occurred in a cooperative single step with a transition midpoint of 5.9 M urea. Unfolding of WT was completely reversible, whereas Q204E failed to fully refold. Prolonged incubation under denaturing conditions led to aggregation, which was also more pronounced for Q204E dimers than for WT. Truncation of 41 residues from the N-terminus or 47 and 5 residues from the N- and C-termini did not affect stability. These studies indicated that a single-site deamidation could significantly diminish the stability of lens βB1-crystallin, supporting the idea that such modifications may play an important role in age-related cataract formation.

Crystallins are the major structural proteins in the lens of the eye. They are highly organized and maintained with little turnover throughout the lifetime of the host (*1*). The important physiological characteristic of crystallins is maintenance of lens transparency by the short-range spatial order (*2*). Therefore, any modification that disrupts this order may be detrimental for lens function.

Crystallins in the mammalian lens are divided into three major classes: α, β, and γ (reviewed in ref *1*). α-Crystallins form very large oligomers (~800 kDa) comprised of 20 kDa subunits and have chaperone-like activity (*3*). β-Crystallins exist as oligomers ranging from 200 to 50 kDa. γ-Crystallins are 21 kDa monomers and share a two-domain folding structure with the β-crystallins. The difference between β- and γ-crystallins is the presence of N-terminal extensions on the β-crystallin subunits. This suggests a possible role of the N-terminal extensions in oligomerization of β-crystallins.

Lens crystallins are extensively modified during aging. These modifications include truncation of the terminal extensions and deamidation (*4*−*11*). βB1- and βA3-crystallins lose 15 and 22 amino acids, respectively, from their N-terminal extensions in the young human lens (*4*, *12*). More extensive truncation of βB1 occurs during aging between residues 33 and 41 (*4*) and in the water-insoluble crystallins (*9*). The role of the N-terminal extensions is not known, but has been proposed to facilitate interactions with other crystallin subunits (*13*). Loss of the extension may then disrupt these interactions. During cataract formation in animal models, the rate of truncation is increased, leading to insolubilization of crystallins and cataract formation (*14*, *15*).

Deamidation also occurs during aging (*5*−*7*, *16*−*18*) and cataract formation (*10*). Deamidations have been reported in all of the human crystallins, except for a minor component, βB3 (*5*, *6*, *16*). Deamidation at specific residues in γS is associated with human senile cataract (*10*, *19*). The extent of deamidation is greater in the water-insoluble than water-soluble crystallins from clear (*5*, *9*) or cataractous lenses (*19*). Since the amount of insoluble crystallins increases as well during aging (*20*), truncation of extensions and deamidation

† This work was supported in part by National Institutes of Health Grants EY12239 (K.J.L.), EY03600 (T.R.S.), EY07755 (L.L.D.), and RR01008 (J.B.F.) and Core Grant EY 10572, by the Shriner's Hospital for Children Foundation (HPB), and by EU BioMed Grant BMH4-CT98-3895 (N.H.L.).

* To whom correspondence should be addressed at the Department of Oral Molecular Biology, Oregon Health & Science University, 611 S.W. Campus Dr., Portland, OR 97239. Phone: (503) 494-8620. Fax: (503) 494-8918. E-mail: lampik@ohsu.edu.

‡ Oregon State University.

§ Oregon Health & Science University.

|| University of Nijmegen.

⊥ Shriner's Hospital for Children.

▽ Medical College of Wisconsin.

@ These authors contributed equally to this work.

10.1021/bi026288h CCC: $22.00
Published on Web 10/31/2002

may be important factors contributing to senile cataract formation (*10*). To test this theory, the stability of modified βB1s was measured in the present study.

Previously, we have shown that elution of modified βB1s on size exclusion chromatography was unusual for their confirmed oligomer size, suggesting an altered shape (*21*). A deamidation was introduced at glutamine 204 in the C-terminal globular domain of βB1, a site predicted to be in a hydrophobic cluster at the interface between two paired domains (*22*). This deamidation was identified in aged lenses by peptide mapping from two-dimensional electrophoresis (*6*) and recently confirmed using tandem mass spectrometry (*23*). This deamidation further resulted in decreased flexibility of the N-terminal extension as seen by nuclear magnetic resonance (NMR)[1] studies (*24*). These data suggest modified βB1s have altered conformations compared to wild-type βB1 (WT). The stability of these altered structures was initially measured by examining their resistance to precipitation during heating. They were found to be less heat-stable (*24*).

In the present study we have examined urea-induced denaturation/renaturation of WT and modified βB1 using different spectrophotometric techniques. Since both truncation and deamidation occur during aging, it is necessary to investigate their relative significance and whether both modifications would cause a synergistic effect on βB1 stability. Modified βB1s with an in vivo site of deamidation at glutamine 204 (*6*) and cleavage between residues 41 and 42 (*4*) were recombinantly expressed, and a truncated βB1 missing part of the N- and C-termini was generated (*21*). The goal of this study was to determine how the stability of βB1 would be affected by deamidation and/or truncation as measured by urea-induced denaturation.

EXPERIMENTAL PROCEDURES

Expression and Purification of Proteins. WT and Q204E were expressed in *E. coli* and purified as described previously (*21*). Truncation of purified WT and Q204E was generated by calpain II (Calbiochem, San Diego, CA) in the presence of 2 mM Ca^{2+}. After a 1−2 h incubation at 37 °C, the reaction was stopped by exchanging the buffer for one lacking Ca^{2+} at 4 °C. A truncated βB1 missing 41 amino acids from the N-terminus (βB1(ΔN41)) found in vivo was also recombinantly expressed as described previously (*4*, *25*).

Electrophoresis, Mass Spectrometry, and Sequence Analysis of Truncated WT (trWT) and Truncated Q204E (trQ204E). Electrophoresis was performed using precast 10% polyacrylamide minigels (NuPAGE, Invitrogen, Carlbad, CA). Proteins were visualized by staining with Coomassie blue G-250 (SimplyBlue SafeStain, Invitrogen). Mass spectrometry was performed to confirm the truncation sites. Approximately 0.17 nmol of trWT and trQ204E was injected into a C18 reversed-phase column in line with an electrospray ionization mass spectrometer (ESI-MS; model LCQ, ThermoFennigan, San Jose, CA). The accuracy of mass determinations within an error of 0.01% was confirmed using horse myoglobin as a standard. The N-terminal amino acid sequence analysis was performed in the Genomics and Proteomics Facility at the University of Oregon (Eugene, OR).

Circular Dichroism (CD). CD spectra of trWT and trQ204E (0.48 mg/mL) were recorded on a JASCO J-500 A spectrometer (JASCO, Easton, MD) in the far-UV range. To remove autolyzed peptides of calpain II, samples were applied to a size exclusion column, 7.5 mm × 30 cm TSK G3000SWXL (TosoHaas, Montgomeryville, PA), equilibrated with 5 mM NaH_2PO_4, 5 mM Na_2HPO_4, 100 mM NaCl, pH 6.8. The samples were then dialyzed against the same buffer containing 100 mM NaF instead of NaCl. CD measurements were taken in a 0.1 mm cell at 20 °C. Secondary structure was calculated using the variable-selection method (*26*). Protein concentration was determined by amino acid analysis.

For the urea stability study, CD spectra of full-length WT and Q204E were measured on an AVIV 202 CD spectrometer (Protein Solutions, Lakewood, NJ) from 200 to 260 nm. A 10 μM sample of protein (280 μg/mL) was tested in various concentrations of urea for unfolding/refolding studies as described in Fluorescence Spectrometry.

Fluorescence Spectrometry. To study the stability of WT and other modified βB1s, fluorescence spectrometry was used to measure protein unfolding and refolding patterns in urea. Proteins at 1 μM (27.9 μg/mL for WT and Q204E, 23.0 μg/mL for trWT and trQ204E) were incubated in varying urea concentrations ranging from 0 to 7 or 8 M. A stock solution of 9 M urea was deionized and filtered, and a stock solution of 10× phosphate buffer was made. Sample buffers were made up by combining the two stock solutions to yield a final concentration of 5 mM Na_2HPO_4, 5 mM NaH_2PO_4, 100 mM NaCl, pH 6.8. Proteins were incubated in urea buffer overnight at 25 °C to ensure equilibrium in urea had been reached. For refolding experiments, protein samples were incubated in 7 M urea buffer overnight and then diluted with phosphate buffer to the desired end concentration of urea.

Fluorescence measurements were made on a Photon Technology International QM-2000-7 spectrofluorimeter (Photon Technology International, Lawrenceville, NJ). The absorption scan was measured between 240 and 320 nm, and the emission wavelength was set at 336 nm. For emission scanning, proteins were excited at 283 nm, and the fluorescence emission was recorded between 300 and 400 nm at 25 °C with the excitation and emission slit width set to 2 nm. Fluorescence measurements were analyzed with FeliX, fluorescence analysis software (Photon Technology International). The fluorescence emission spectrum was corrected by subtracting the blank buffer spectrum for each urea concentration and smoothed using the Savitzky−Golay equation.

Fluorescence measurements for βB1(ΔN41) were taken using a Shimadzu RF-5301 PC spectrofluorimeter (Shimadzu, Kyoto, Japan). Emission spectra were measured between 300 and 400 nm (0.2 nm interval) with an excitation wavelength of 285 nm. For the measurement of unfolding, an excitation wavelength of 285 nm and an emission

[1] Abbreviations: NMR, nuclear magnetic resonance; WT, wild-type βB1-crystallin; Q204E, deamidated βB1-crystallin; βB1(ΔN41), truncated βB1-crystallin missing 41 residues from the N-terminus; trWT, truncated βB1-crystallin missing 47 residues from the N-terminus and 5 residues from the C-terminus; trQ204E, truncated and deamidated βB1-crystallin missing 47 residues from the N-terminus and 5 residues from the C-terminus; βB1(ΔN41), truncated βB1-crystallin missing 41 residues from the N-terminus; CD, circular dichroism; ESI-MS, electrospray ionization mass spectrometer; EPR, electron paramagnetic resonance; MTSL, methanethiosulfonate spin label; SDS−PAGE, sodium dodecyl sulfate−polyacrylamide gel electrophoresis; SDSL, site-directed spin labeling.

wavelength of 350 nm were used. The protein concentration was 0.05 mg/mL in phosphate buffer (60 mM Na_2HPO_4, 40 mM NaH_2PO_4, pH 7.0) and urea at concentrations varying between 0 and 8.5 M. Samples were diluted using a 10 M urea stock solution.

Folding Calculations. The percent folded protein was calculated from fluorescence and CD data by the following equation:

$$\% \text{ folded protein} = (V_i - V_u)/(V_n - V_u) \times 100$$

where V_i is the data value at each urea concentration, V_u is the data value at the highest urea concentration, and V_n is the data value for native protein without urea. For fluorescence data, fluorescence intensity at 357 nm was used, and for CD measurements, ellipticity at 218 nm was used. These wavelengths were chosen because they produced the largest difference between native and unfolded proteins. After the data were plotted, curves were fitted with Origin (Microcal Software, Inc., Northhampton, MA) using the nonlinear sigmoidal-curve-fitting tool with the Boltzmann function or a modified Boltzmann function. The urea concentration at 50% unfolding was calculated from the curve-fit equations as a parameter.

Electron Paramagnetic Resonance Spectrometry (EPR). Samples for EPR analysis were spin labeled using the methanethiosulfonate spin label (MTSL; Toronto Research Chemicals, Inc., Ontario, Canada) by incubating protein overnight at 4 °C with a 10-fold molar excess of the spin label. Excess label was removed by exhaustive dialysis, and samples were concentrated to 3.0 mg/mL. Samples (20 μL total volume) were contained in 50 μL glass capillaries placed in a standard 2 mm EPR tube, and contained a final protein concentration of 0.75 mg/mL in 10 mM phosphate, 100 mM NaCl, pH 7.2. EPR spectra were obtained on a Varian E-109 spectrometer (Varian, Palo Alto, CA) at 10 mW incident microwave power with a 1.0 G field modulation. Data acquisition and analysis were carried out with software written in LabView by C. Altenbach. Rotational correlation times were estimated on the basis of the outermost hyperfine splittings (*27*) using the tensor parameters $g_{xx} = 2.0076$, $g_{yy} = 2.0050$, $g_{zz} = 2.0023$, $A_{xx} = 6.2$G, $A_{yy} = 5.9$G, and $A_{zz} = 37$G (*28*).

Quantitation of the fraction of denatured protein, f_d, at a given urea concentration was done as previously described (*29*). Briefly, a difference spectrum was generated by digital subtraction of an appropriate amount of the EPR spectrum obtained in 6 M urea until a line shape similar to that of the native spectrum (in the absence of urea) was obtained. Integrated intensities before and after subtraction were then compared. In general, difference spectra could be obtained that were essentially identical to the native spectra. For a two-state equilibrium between denatured and native protein

$$K_{dn} = f_d/f_n \quad (1)$$

The Gibbs free energy of unfolding, ΔG_u, at any denaturant concentration is

$$\Delta G_u = -RT \ln K_{dn} \quad (2)$$

where f_n is the fraction of native protein, R the gas constant, and T the absolute temperature. For two-state systems it has been well-established that ΔG_u varies linearly with denaturant concentration, such that

$$\Delta G_u^\circ = \Delta G_u + m[\text{urea}] \quad (3)$$

where m is the slope of a linear extrapolation of the dependence of unfolding on denaturant concentration (see Figure 10) and ΔG_u° is the reference-state Gibbs free energy of unfolding in the absence of denaturant (*29*−*31*). Denaturation curves (Figure 9) and linear extrapolations (Figure 10) were fitted by standard nonlinear and linear least-squares regression methods using the Origin software package. It has been suggested that the midpoint of the equilibrium transition, C_m, may be a more reliable experimental parameter than the extrapolated intercept (*31*, *32*). At 50% denaturation, $\Delta G_u^\circ = mC_m$, providing an alternate method for determination of ΔG_u°. In this study we found excellent agreement between free energies of unfolding calculated by these two methods.

RESULTS

Secondary Structure of Truncated βB1-Crystallins. To investigate how the removal of the N- and C-terminal extensions affects the structure and stability of βB1-crystallins, WT and Q204E βB1s were proteolyzed by calpain II in the presence of 2 mM calcium. Previously, it was reported that calpain II truncates 47 residues from the N-terminus and 5 residues from the C-terminus of WT βB1 (*21*), which results in trWT with a calculated mass of 23040.8 and corresponds within experimental error to what was observed in this study (small panel, Figure 1B). On SDS−PAGE both trWT and trQ204E migrated to similar positions between the 20 and 25 kDa standards (Figure 1A), suggesting the same cleavage of the two proteins by calpain II. The mass of trQ204E was 23043.9 (Figure 1B), which corresponded to the predicted mass of Q204E βB1 missing 47 amino acids from the N-terminus and 5 from the C-terminus (calculated mass of 23041.8). Protein N-terminal sequencing confirmed that the amino acids on the new N-terminus corresponded to residues starting at alanine 48 for trQ204E as was previously determined for trWT (*21*).

Circular dichroism measurements were performed to investigate the secondary structure of trWT and trQ204E (Figure 2). The data for full-length βB1-crystallins were included for comparison (*21*). The spectra showed double minima at 205 and 215 nm, characteristic of both α-helical and β-pleated sheet conformation as was previously reported for full-length βB1 and bovine β-high crystallins (*21*, *33*). The average secondary structure for trWT was 10% α-helix, 41% β-structure, 20% turns, and 29% other structures, and for trQ204E, 9% α-helix, 42% β-structure, 19% turns, and 29% other structures. These results indicated that the two proteins have very similar secondary structure. Compared to their respective full-length proteins (see the inset, Figure 2; *21*), the α-helical content of the truncated proteins was lower. The CD spectrum of a recombinantly expressed truncated protein, βB1(ΔN41), also showed double minima and a lower overall content of α-helical structure (data not shown).

Absorption and Emission Spectra of βB1. Spectrofluorimetry was used to measure structural changes of proteins during urea-induced denaturation. The UV absorption spec-

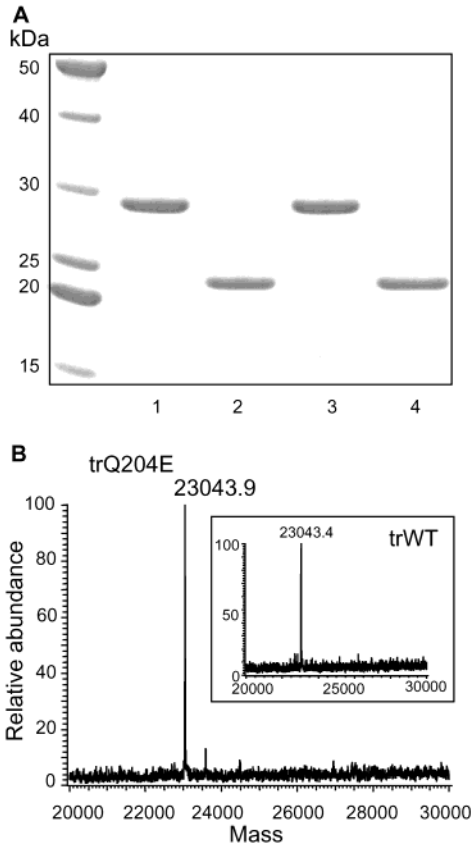

FIGURE 1: Truncation of βB1-crystallins: (A) SDS−PAGE of WT (1), trWT (2), Q204E (3), and trQ204E (4); (B) electrospray ionization mass spectra of trQ204E and trWT (insertion).

trum of WT showed maximum absorbance at 283 nm and a shoulder at 290 nm (Figure 3). Thus, the excitation wavelength was set at 283 nm for the fluorescence emission scan. WT showed a maximum fluorescence emission at 336 nm. Q204E, trWT, and trQ204E had similar absorption and emission spectra compared to WT. However, the absorption and emission intensities were different among the four proteins at a 1 μM protein concentration. The order of fluorescence intensity from highest to lowest was Q204E, WT, trQ204E, and trWT (data not shown).

Fluorescence Emission Spectra of Unfolding βB1-Crystallin. To study the stability of βB1-crystallins in a denaturing environment, the proteins at 1 μM were incubated in various concentrations of urea. Protein unfolding/refolding was detected by measuring fluorescence emission due to aromatic residues likely dominated by eight tryptophan residues. Fluorescence emission spectra in increasing concentrations of urea showed a red shift as the maximum fluorescence wavelength increased from 336 to 353 nm (data shown for WT, Figure 4), indicating protein unfolding. As denaturation progressed in increasing urea concentrations, the fluorescence intensity increased. Full denaturation occurred only at high concentrations of urea, ≥7 M (Figures 5−7). Higher concentrations of protein, 18 μM, showed the same pattern of denaturation in urea as 1 μM (data not shown).

Unfolding/Refolding of WT and Q204E. Fluorescence emission was compared between WT and Q204E at 357 nm, where the maximum difference was observed between native and fully denatured βB1 emission spectra, and the percent folded protein curves were generated (Figure 5). As the

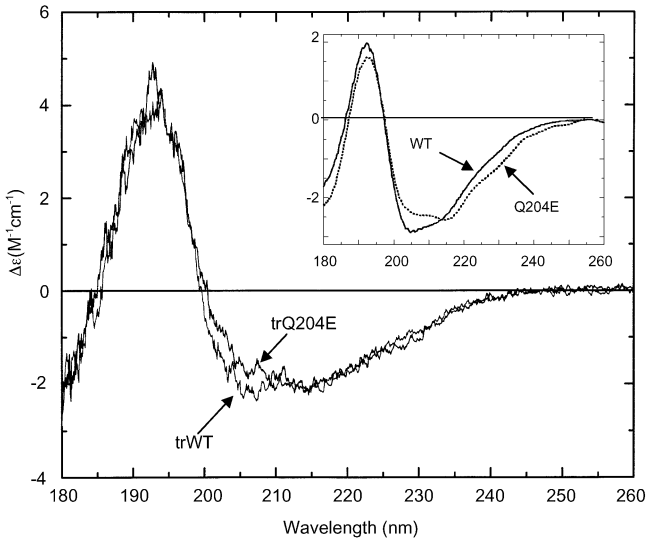

FIGURE 2: Circular dichroism of truncated βB1-crystallins. Samples of 20 μM (0.48 μg/mL) trWT and trQ204E were used for CD measurements. The inset shows full-length WT (—) and Q204E (---) CD from the previous publication for comparison purposes. The inset is reprinted with permission from ref *21*. Copyright 2001 Elsevier Science.

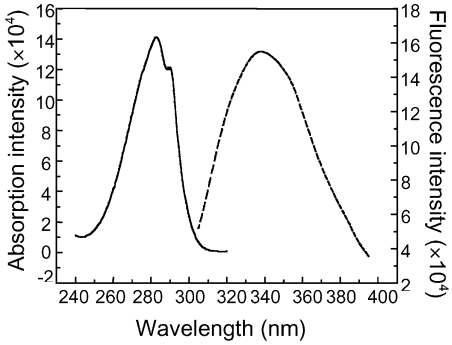

FIGURE 3: Absorption (—) and emission (---) spectra of WT βB1. A 1 μM (27.9 μg/mL) sample of WT was used. For the UV absorption spectrum, absorbance was measured from 240 to 320 nm with emission wavelength at 336 nm. For the fluorescence emission spectrum, the protein was excited at 283 nm and the emission was measured from 300 to 400 nm.

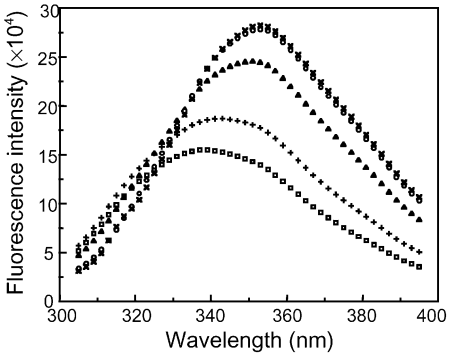

FIGURE 4: Urea-induced denaturation of WT βB1 as measured by fluorescence spectroscopy. A 1 μM sample of WT was incubated in various concentrations of urea overnight at 25 °C: 0 M urea, □; 3 M, +; 5 M, △; 6.5 M, ○; 7.5 M, ×. The fluorescence emission was measured from 300 to 400 nm with excitation at 283 nm.

denatured proteins refolded, renaturation curves as determined by fluorescence were superimposable on those obtained during unfolding. This indicated reversible protein

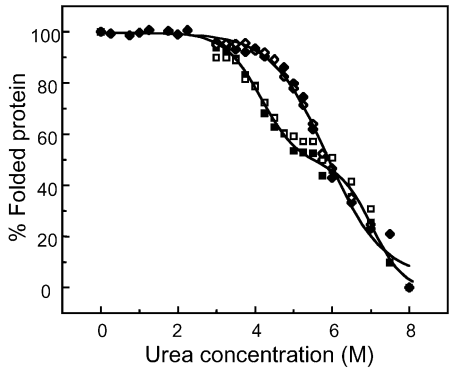

FIGURE 5: Stability of WT and Q204E βB1-crystallins in urea measured by fluorescence. Unfolding (filled symbols) and refolding (open symbols) of WT (tilted squares) and Q204E (squares) were monitored by fluorescence spectroscopy. Protein (1 μM) was excited at 283 nm, and the fluorescence emission intensity at 357 nm was used for the graph.

denaturation and renaturation in urea. A decrease in folded protein was observed starting at 3 M urea for Q204E and 4 M urea for WT. WT showed a one-step transition yielding 50% unfolding at 5.9 M, whereas Q204E showed a two-step transition with transition midpoints at 4.1 and 7.2 M urea (Figure 5).

CD measurements of the unfolding of WT (Figure 6A) and Q204E (Figure 6B), obtained by following ellipticity at 218 nm, were almost identical to the fluorescence data. The 50% unfolding for WT was at 5.9 M. For Q204E two transitions were observed with midpoints at 4.2 and 7.1 M urea. However, in contrast to the fluorescence data, Q204E was not able to refold completely when the denatured protein was diluted in buffer without urea, whereas the unfolding and refolding curves from WT spectra were superimposable. Figure 6C shows that refolded Q204E at 3 M urea is more denatured than that obtained during the initial unfolding. These differences suggested the possibility of aggregation by Q204E under denaturing conditions at the higher protein concentrations used in the CD experiments (10 μM) as compared to fluorescence (1 μM).

Unfolding/Refolding of Truncated βB1-Crystallins. To investigate whether truncation of the extensions would influence the stability of βB1, the N- and C-terminal extensions from WT and Q204E were cleaved by calpain II. Both trWT and trQ204E showed a reversible denaturation measured by fluorescence (Figure 7). Truncation of extensions did not change the stability of the proteins compared to full-length proteins. Similar to the full-length protein, trWT underwent 50% unfolding at 5.8 M urea with a one-step transition. The denaturation curve of βB1(ΔN41) was superimposable on that of full-length βB1 (data not shown). TrQ204E showed a two-step transition with midpoints at 4.1 and 6.5 M. The second transition of trQ204E was at a lower urea concentration compared to that of full-length Q204E (7.2 M).

Denaturation of the N-Terminal Domain. The fluorescence and CD data described above reflect the overall denaturation of the entire βB1 molecule. To investigate unfolding in a selected region of βB1, we employed site-directed spin labeling (SDSL) of cysteine 79. This native cysteine, by analogy to βB2-crystallin (*1*), is located in the N-terminal globular domain and thus is well separated from the

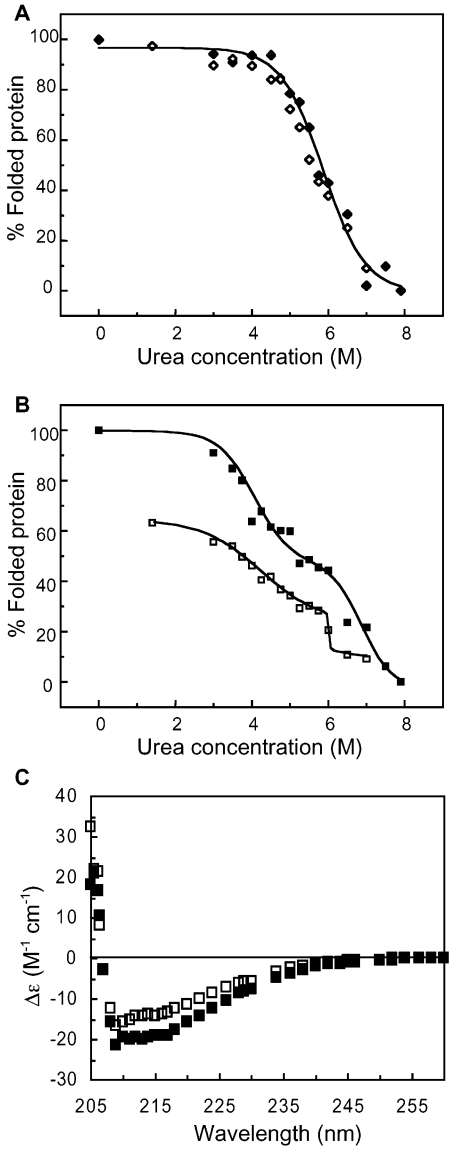

FIGURE 6: Stability of WT and Q204E βB1-crystallins in urea measured by CD. Unfolding (filled symbols) and refolding (open symbols) of WT (tilted squares) and Q204E (squares) were monitored by CD. Samples of 10 μM proteins were used, and the ellipticity at 218 nm was used for the graph. (A) Urea denaturation curve of WT. (B) Urea denaturation curve of Q204E. (C) Whole spectra of unfolding and refolding Q204E in 3 M urea.

deamidation site. The rotational mobility of the nitroxide spin label attached at Cys 79 reports selectively on the local environment (see refs *34* and *35* for reviews), and thus on the loss of tertiary and/or quaternary structure at that site (*29*, *36*). On the basis of homology to the βB2 structure, Cys 79 is predicted to be in a loop within the first Greek key motif of the N-terminal domain (*37*). However, in βB2 the Cys is between two prolines, whereas in βB1 the Cys is between a glutamate and a serine.

EPR spectra of MTSL-labeled WT and Q204E after a 30 min incubation at ambient temperature (~22 °C) in various concentrations of urea are shown in Figure 8. The uppermost (control) spectra taken in the absence of urea were essentially identical, both indicating that the spin-label side chain was attached at Cys 79 residues in a buried environment with interactions that limit the rotational motion of the nitroxide. During the initial denaturation phase, both samples retained

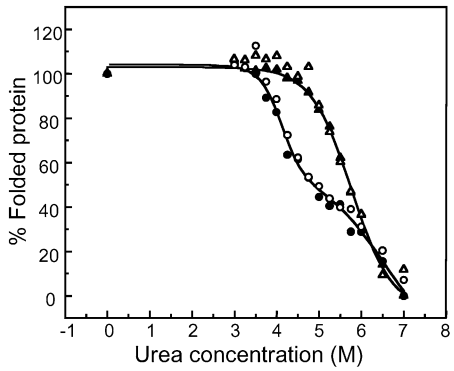

FIGURE 7: Stability of trWT and trQ204E βB1-crystallins in urea. Unfolding (filled symbols) and refolding (open symbols) of trWT (triangles) and trQ204E (circles) were monitored by fluorescence spectroscopy. The same conditions were used as described in Figure 5. For truncation of WT and Q204E, proteins were incubated with calpain II in buffer containing 2 mM Ca^{2+} at 37 °C for 1−2 h.

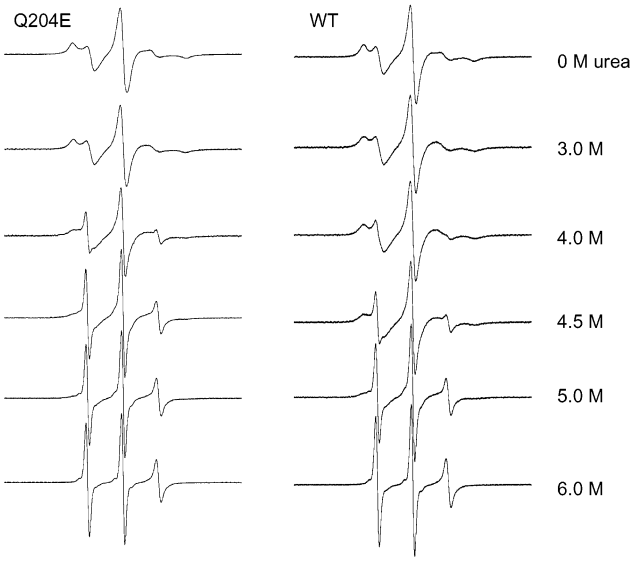

FIGURE 8: EPR spectra of Q204E (left) and WT (right) βB1-crystallins as a function of urea concentration. Samples containing 0.75 mg of protein/mL and the indicated final concentration of urea were incubated for 30 min at room temperature (22 °C) before the spectra were recorded. Samples contained (from top to bottom) 0, 3.0, 4.0, 4.5, 5, and 6 M urea. Spectra were signal averaged 8−10 times each, with a scan width of 100 G.

the native structure at the spin-label site up to 3 M urea. Beginning at approximately 3.5 M urea, addition of increasing concentrations of denaturant resulted in the appearance of three narrow lines arising from a population of spin labels with relatively free rotational mobility (Figure 8). Denaturation at Cys 79 was complete at 6 M urea, with no further changes at 7 M being observed for either WT or Q204E.

Quantitation of the fraction of denatured protein (see the Experimental Procedures) yielded the denaturation curves shown in panels A and B of Figure 9. Both curves are indicative of highly cooperative denaturation, with unfolding occurring over a relatively narrow range of urea concentrations, and both fit well to a two-state equilibrium model (solid lines in Figure 9). The unfolding of Q204E occurred at lower denaturant concentrations than for WT, with midpoints of the transitions (C_m) of 4.62(±0.02) and 4.88(±0.03) M urea for Q204E and WT, respectively. The dependence of the free energy of unfolding (eq 2) on urea concentration is shown

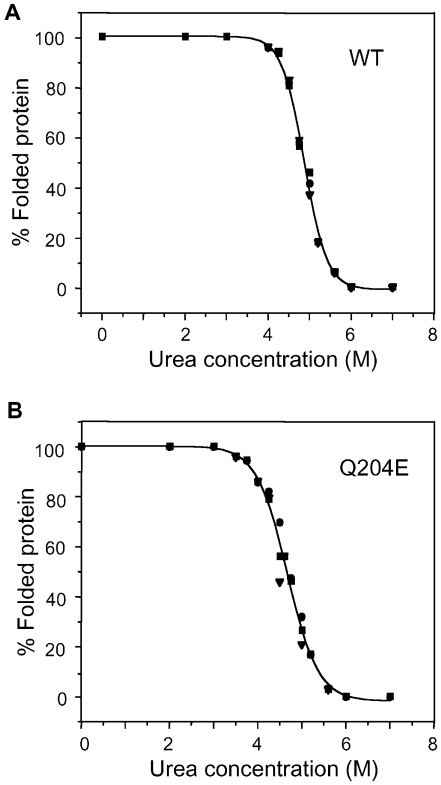

FIGURE 9: Urea denaturation curves for WT (A) and Q204E (B) βB1-crystallins derived from EPR data taken after 30 min of incubation at room temperature. Midpoints of the transitions occur at 4.88 and 4.62 M urea for WT and Q204E, respectively. The percent denaturation was determined by double integration of the spectra after the rotationally mobile component had been removed by subtraction of spectra obtained with 6 M urea as the fully denatured reference (see Figure 8). Different symbols represent independent experiments.

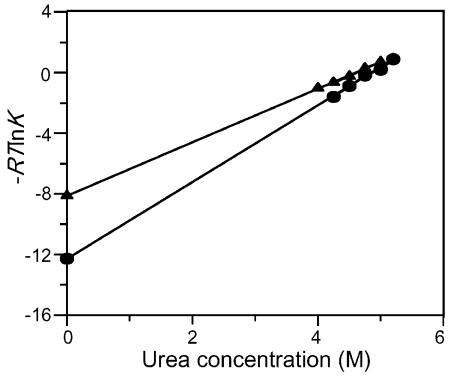

FIGURE 10: Free energy of denaturation for the N-terminal domain region surrounding Cys 79. *RT* ln *K* values were calculated for $K = f_d/f_n$ from the transition region of the urea denaturation curves for WT (circles) and Q204E (triangles). Extrapolation by linear regression analysis to zero denaturant gives an estimate of the free energy of unfolding in the absence of urea.

in Figure 10. Linear extrapolation to zero denaturant concentration yielded free energies of unfolding, $\Delta G_u°$, of 12.3(±0.7) kcal/mol for WT and 8.1(± 0.3) kcal/mol for Q204E. Free energies of unfolding calculated from the midpoints of the transitions and the slopes of the linear extrapolations (*31*, *32*) were 12.30 and 8.13 kcal/mol for WT and Q204E, respectively.

Extended incubation of samples containing intermediate amounts of denatured protein led to the formation of a

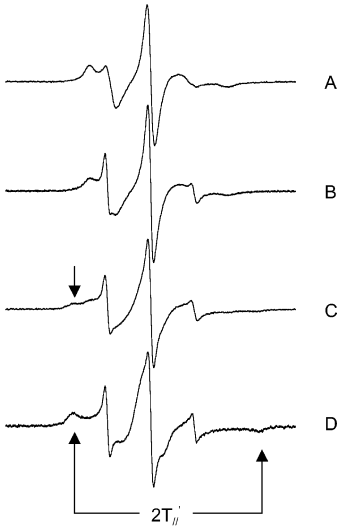

FIGURE 11: Prolonged incubation under denaturing conditions leads to protein aggregation. EPR spectra of Q204E are shown in the absence of urea (A) and in 4.25 M urea (B) after 30 min, (C) 2 h, and (D) 24 h of incubation at 22 °C. The arrow in (C) indicates the appearance of a strongly immobilized component due to aggregation, with an outer hyperfine splitting ($2T_{\parallel}'$) of 62 G as indicated in (D).

strongly immobilized component in the EPR spectrum with outer hyperfine splittings ($2T_{\parallel}'$) of approximately 62 G (Figure 11), as compared to 46 G in the native state. These splittings correspond to rotational correlation times of 6.8 and 2.9 ns, respectively (*27*), indicating an increase in the rotational radius of approximately 35%. This decrease in the overall rotational motion could reflect increased protein−protein interactions (i.e., formation of tetramers or higher aggregates) as observed by light scattering upon heat-induced denaturation of βB1 (24), although changes in the shape of the βB1 dimer cannot be ruled out. For Q204E, this spectral component became evident after 2 h for samples containing between 4 and 5 M urea, and at 3 M urea in samples incubated overnight. Higher concentrations of urea (>5.2 M) maintained the protein in the fully unfolded state. In contrast, for WT this strongly immobilized component was only observed after 24 h at urea concentrations between 4 and 5 M. Remarkably, WT samples containing ≤3 M urea were found to be stable at ambient temperature for up to 10 days.

DISCUSSION

Deamidation of βB1-Crystallin Decreases Stability. Our studies indicated that a single-site deamidation of βB1-crystallin decreases its stability during urea-induced denaturation. Denaturation curves derived from both fluorescence and CD measurements showed similar results; in both cases, Q204E unfolded at lower urea concentrations than WT and the deamidated mutant exhibited a two-step transition. This decreased stability upon deamidation is a potentially important event that could ultimately alter protein−protein interactions and contribute to loss of clarity in the lens.

Previous studies using thermal denaturation indicated that deamidation also causes an increased susceptibility to aggregation (*24*). This may explain our observation that, unlike WT, Q204E did not completely refold in CD experiments (Figure 6C). The increased susceptibility to aggregation and/or irreversible denaturation is further supported by our EPR data indicating a greater tendency of Q204E to possibly form higher molecular weight species upon prolonged incubation under denaturing conditions (Figure 11).

In contrast to CD and fluorescence data, results from EPR spin-labeling studies report specifically on the local tertiary and quaternary structure in the region of Cys 79. By homology to the βB2 structure, Cys 79 is located in a loop of the N-terminal domain (*37*). In addition, these studies were also conducted at a concentration where βB1 is almost entirely in the dimeric oligomerization state (*21*). Thus, it is not surprising that the unfolding transitions occurred at different urea concentrations compared to those observed using CD or fluorescence. Indeed, $\Delta G_u°$ values determined by EPR spin-labeling methods are highly specific for the site examined, and can vary significantly even among residues in relatively close proximity (*36*). Despite these differences, the EPR data also indicated that Q204E is destabilized relative to WT. Noteworthy is that destabilization was observed at a site in the N-terminal domain, even though the deamidation site was in the C-terminal domain.

Our EPR studies showing destabilization at a site in the N-terminal domain upon deamidation in the C-terminal domain suggested the presence of structural interactions between the two domains. These interactions may be intramolecular between the two domains of a given monomer, intermolecular between domain-swapped regions in the dimer (as observed for βB2; *37*), or both. Such interactions may contribute to the remarkable stability of the crystallins, which must exist with very little turnover in the lens. Both β- and γ- crystallins have two domains comprised of two Greek key motifs (reviewed in ref *38*). The γ-crystallins exist as monomers with the two domains being paired, while βB2 forms a dimer with the opposite domains pairing to form a domain-swapped dimer (*38*). Nonetheless, interactions between the domains are similar for the γ-crystallins and βB2, and are important for stability. Replacing an alanine with an aspartic acid in the N-terminal domain of γB destabilized the C-terminal domain (*39*). Mutations in one domain can affect the stability of the other. The relative contributions of inter- vs intradomain interactions to βB1 stability remain to be determined.

In βB2-crystallin, the N- and C-terminal domains are topologically similar. Yet, recombinant expression of the individual domains showed that the N-terminal domain unfolded at a lower urea concentration (*40*). Our EPR studies are consistent with the N-terminal domain being less stable than the C-terminal domain, although additional sites in each domain must be examined before any definitive conclusion can be reached.

Deamidation of βB1 also led to the formation of an intermediate state during unfolding not seen for WT, as indicated by the two-step denaturation curve observed for Q204E. This may reflect alterations in domain−domain interactions. This is consistent with a direct interaction between Gln 204 and the N-terminal domain as predicted from the βB2 structure (*22*).

Alternatively, the enhanced aggregation of deamidated βB1 following unfolding (*24*) may perturb the folding−unfolding equilibrium, thus producing an inflection in the denaturation curve. Aggregation would also preclude refolding of Q204E, as observed by CD (Figure 6). Our current EPR data also suggest that protein−protein aggregation may

occur upon prolonged incubation of samples containing denatured protein (Figure 11), and as with heat-induced denaturation (*24*), this was more pronounced for Q204E relative to WT.

Extensions on βB1-Crystallins Do Not Affect Stability. Another important finding from the current study was that loss of the N- and C-terminal extensions did not alter the apparent stability of βB1. Our fluorescence and CD data indicated that the Greek key domains of βB1 were maintained even in the absence of the terminal extensions, with trWT and trQ204E both showing very similar denaturation patterns in urea compared to their full-length proteins. We have also observed that loss of the WT βB1 extensions does not decrease its heat stability (*24*). Our findings support those of Coop et al. showing that an altered N-terminal extension sequence or deletion of 16 amino acids from the C-terminal extension did not change the heat stability of chick βB1 (*41*). Similarly, the extensions of βB2 were observed to be flexible and, thus, judged not to be involved in stabilizing the dimer (*42*). This suggests that the stability of the domain interactions contributes most to the stability of βB1 monomers and dimers, as has been reported for other members of the β/γ-family (*37*).

Alternatively, the role of the extensions on βB1 may be to facilitate interactions in the β-high assemblies comprised of tetramers and octomers (*6*, *13*). The extensions have also been proposed to serve as spacers preventing the formation of higher homooligomers, but could promote heterooligomers (*42*, *43*). We, along with others, have shown that removal of the extensions of βB1 resulted in delayed elution on size exclusion chromatography, suggesting exposure of interactive sites on the domains (*21*, *25*). We also observed that the extensions in βB1 were critical to maintaining the solubility of βB1−αA-crystallin complex during heating (*24*). These observations indicate that the extensions in βB1 may serve to direct complex interactions with other crystallins, rather than to maintain its intrinsic stability.

In conclusion, these studies demonstrate that a single-site deamidation results in a significant reduction in the stability of βB1-crystallin. Deamidation was found to decrease the stability of βB1 at concentrations at which βB1 would be predominantly either a monomer or a dimer. Our observation of destabilization of the βB1 monomer suggests that deamidation may alter the stability of the N- or C-terminal domains and/or intramolecular interactions between them. If true, this indicates that the domains of βB1 may be more stable or interact more closely than those of βB2, and may partly explain the greater stability of βB1 in urea than what has been reported for βB2 (*40*). The complexity of intermolecular interactions makes the effects of deamidation on the βB1 dimer more difficult to interpret. The destabilization that occurs upon deamidation of βB1 may render it more prone to protein−protein aggregation, and this may contribute to cataract formation in vivo.

ACKNOWLEDGMENT

We thank Dr. Steven King for letting us use the spectrofluorimeter and Debra McMillen for performing N-terminal amino acid sequence analysis at the University of Oregon.

REFERENCES

1. Slingsby, C., and Clout, N. J. (1999) *Eye 13*, 395−402.
2. Delaye, M., and Tardieu, A. (1983) *Nature 302*, 415−417.
3. Derham, B. K., and Harding, J. J. (1999) *Prog. Retinal Eye Res. 18*, 463−509.
4. David, L. L., Lampi, K. J., Lund, A. L., and Smith, J. B. (1996) *J. Biol. Chem. 271*, 4273−4279.
5. Lund, A. L., Smith, J. B., and Smith, D. L. (1996) *Exp. Eye Res. 63*, 661−672.
6. Lampi, K. J., Ma, Z., Hanson, S. R. A., Azuma, M., Shih, M., Shearer, T. R., Smith, D. L., Smith, J. B., and David, L. L. (1998) *Exp. Eye Res. 67*, 31−43.
7. Ma, Z., Hanson, S. R. A., Lampi, K. J., David, L. L., Smith, D. L., and Smith, J. B. (1998) *Exp. Eye Res. 67*, 21−30.
8. Takemoto, L., and Boyle, D. (1998) *Biochemistry 37*, 13681−13685.
9. Hanson, R. A. S., Hasan, A., Smith, D. L., and Smith, J. B. (2000) *Exp. Eye Res. 71*, 195−207.
10. Takemoto, L., and Boyle, D. (2000) *Mol. Vision 6*, 164−168.
11. Takemoto, L. (2001) *Curr. Eye Res. 22*, 148−153.
12. Lampi, K. J., Ma, Z. X., Shih, M., Shearer, T. R., Smith, J. B., and David, L. L. (1997) *J. Biol. Chem. 272*, 2268−2275.
13. Ajaz, M. S., Ma, Z., Smith, D. L., and Smith, J. B. (1997) *J. Biol. Chem. 272*, 11250−11255.
14. David, L. L., Wright, J. W., and Shearer, T. R. (1992) *Biochim. Biophys. Acta 1139*, 210−216.
15. Shearer, T. R., Ma, H., Fukiage, C., and Azuma, M. (1997) *Mol. Vision 3*, 8.
16. Groenen, P. J. T. A., Merck, K. B., de Jong, W. W., and Bloemendal, H. (1994) *Eur. J. Biochem. 225*, 1−19.
17. Hanson, S. R. A., Smith, D. L., and Smith, J. B. (1998) *Exp. Eye Res. 67*, 301−312.
18. Yang, Z., Chamorro, M., Smith, D. L., and Smith, J. B. (1994) *Curr. Eye Res. 13*, 415−421.
19. Veniamin, L. N., Purkiss, A. G., Smith, D. L., and Smith, J. B. (2002) *Biochemistry 41*, 8638−8648.
20. Clark, R., Zigman, S. and Lerman, S. (1969) *Exp. Eye Res. 8*, 172−182.
21. Lampi, K. J., Oxford, J. T., Bachinger, H. P., Shearer, T. R., David, L. L., and Kapfer, D. M. (2001) *Exp. Eye Res. 72*, 279−288.
22. Bax, B., Lapatto, R., Nalini, V., Driessen, H., Lindley, P. F., Mahadevan, D., Blundell, T. L., and Slingsby, C. (1990) *Nature 347*, 776−780.
23. Zhang, Z. (2001) Identification and Characterization of Post-translational Modifications in Human Lens Beta Crystallins During Aging Process, Ph.D. Thesis, University of Nebraska, Lincoln, NE.
24. Lampi, K. J., Kim, Y. H., Bachinger, H. P., Boswell, B. A. Lindner, R. A., Carver, J. A., Shearer, T. R., David, L. L., and Kapfer, D. M. (2002) *Mol. Vision 8*, 359−366.
25. Bateman, O. A., Lubsen, N. H., and Slingsby, C. (2001) *Exp. Eye. Res. 73*, 321−331.
26. Compton, L. A., Mathews, C. K., and Johnson, W. C., Jr. (1987) *J. Biol. Chem. 262*, 13039−13043.
27. Freed, J. H. (1976) in *Spin Labeling Theory and Applications* (Berliner, L. J., Ed.) pp 53−121, Academic Press, New York.
28. Columbus, L., Kálai, T., Jekõ, J., Hideg, K., and Hubbell, W. L. (2001) *Biochemistry 40*, 3828−3846.
29. Klug, C. S., Su, W., Liu, J., Klebba, P. E., and Feix, J. B. (1995) *Biochemistry 34*, 14230−14236.
30. Pace, C. N. (1986) *Methods Enzymol. 131*, 266−280.
31. Kellis, J. T., Jr., Nyberg, K., and Fersht, A. R. (1989) *Biochemistry 28*, 4914−4922.
32. Serrano, L., Horovitz, A., Avron, B., Bycroft, M., and Fersht, AR. (1990) *Biochemistry 29*, 9343−9352.
33. Bloemendal, M., Toumadje, A., and Johnson, W. C., Jr. (1999) *Biochim. Biophys. Acta 1432*, 234−238.
34. Feix, J. B., and Klug, C. S. (1998) in *Biological Magnetic Resonance* (Berliner, L., Ed.) Vol. 14, pp 251−281, Plenum Press, New York.
35. Hubbell, W. L., Cafiso, D. S., and Altenbach, C. (2000) *Nat. Struct. Biol. 7*, 735−739.
36. Klug, C. S., and Feix, J. B. (1998) *Protein Sci. 7*, 1469−1476.
37. Lapatto, R., Nalini, V., Bax, B., Driessen, H., Lindley, P. F., Blundell, T. L., and Slingsby, C. (1991) *J. Mol. Biol. 222*, 1067−1083.
38. Jaenicke, R., and Slingsby, C. (2001) *Crit. Rev. Biochem. Mol. Biol. 36*, 435−499.
39. Palme, S., Slingsby, C., and Jaenicke, R. (1997) *Protein Sci. 6*, 1529−1536.
40. Wieligmann, K., Mayr, E.-M., and Jaenicke, R. (1999) *J. Mol. Biol. 286*, 989−994.

41. Coop, A., Goode, D., Sumner, I., and Crabbe, M. J. (1998) *Graefe's Arch. Clin. Exp. Ophthalmol. 236*, 146−150.
42. Slingsby, C. And Bateman, O. A. (1990) *Biochemistry 29*, 6592−6599.
43. Trinkl, S., Glockshuber, R., and Jaenicke, R. (1994) *Protein Sci. 3*, 1392−1400.

BI026288H